

# Application of the DSMC and NS Techniques to the Modeling of a Dense, Low Reynold's Number MEMS Device

E.V. Titov and D.A. Levin

*Pennsylvania State University,  
University Park, PA 16802*

**Abstract.** The modeling of micro flows through a 3D micro nozzle was investigated by means of the DSMC and NS techniques in order to verify the influence of the computational scheme parameters on the predicted flow quantities. The investigated low Reynold's number flow has a complex structure containing subsonic and supersonic parts. Since the influence of the boundary layer on the flow characteristics is significant, a strong effort was made to predict the boundary layer structure as exactly as possible.

## 1. INTRODUCTION

MEMS-based propulsion devices are under development in order to deliver precise impulses for spacecraft maneuvers Ref. [1]. The advantages of these propulsion devices include lightweight materials and the ability to provide versatile thrust levels along with the potential of clustering of such thruster devices. A wide range of phenomena which are specific to the MEMS functionality has been considered in Ref. [2] including DSMC investigations of the nozzle flow taking into account the removal of energy from the flow by heat transfer to the nozzle wall. Several conclusions were obtained from this work. In particular it was found that a strong influence of the three dimensionality on the predicted flow properties takes place due to the specifics of the nozzle geometry.

In the current work, a strong effort is undertaken in order to study two particular 3D cases of a similar MEMS flow. The main purpose of the work is to obtain an independence of the calculated flow quantities from the numerical scheme parameters for both cases. The cases are similar except for the stagnation pressure levels. Both DSMC and NS numerical schemes were used for low pressure case and NS scheme was used for high pressure case.

## 2. NOZZLE GEOMETRY AND FLOW CONDITIONS

The geometry of the micro nozzle considered in this work is the same as developed by NASA Glenn researchers. A configuration of the nozzle can be seen in Fig 1. where a schematic of the 3D computational domain for a series of Navier Stokes (NS) calculations is presented. The internal dimensions of the nozzle are presented in the Table 1. The high-temperature flow inside the micro truster is generated by a laser-ignited solid mono-propellant decomposition. Molecular nitrogen, the major product of such a decomposition, is considered in the current studies. Two different stagnation pressures of 0.1 and 5 atm are studied. The stagnation temperature remains equal to 2,000 K for both cases and the wall temperature is fixed at 300 K.

Since the nozzle flow is viscous and for a stagnation pressure of 0.1 atm, portions of the flow will be in the transitional regime, a kinetic technique must be employed to accurately predict the device parameters in this case. On the other hand, current research activities are aimed at increasing the device performance by increasing the

# Report Documentation Page

*Form Approved*  
*OMB No. 0704-0188*

Public reporting burden for the collection of information is estimated to average 1 hour per response, including the time for reviewing instructions, searching existing data sources, gathering and maintaining the data needed, and completing and reviewing the collection of information. Send comments regarding this burden estimate or any other aspect of this collection of information, including suggestions for reducing this burden, to Washington Headquarters Services, Directorate for Information Operations and Reports, 1215 Jefferson Davis Highway, Suite 1204, Arlington VA 22202-4302. Respondents should be aware that notwithstanding any other provision of law, no person shall be subject to a penalty for failing to comply with a collection of information if it does not display a currently valid OMB control number.

1. REPORT DATE <b>13 JUL 2005</b>	2. REPORT TYPE <b>N/A</b>	3. DATES COVERED <b>-</b>	
4. TITLE AND SUBTITLE <b>Application of the DSMC and NS Techniques to the Modeling of a Dense, Low Reynold's Number MEMS Device</b>		5a. CONTRACT NUMBER	
		5b. GRANT NUMBER	
		5c. PROGRAM ELEMENT NUMBER	
6. AUTHOR(S)		5d. PROJECT NUMBER	
		5e. TASK NUMBER	
		5f. WORK UNIT NUMBER	
7. PERFORMING ORGANIZATION NAME(S) AND ADDRESS(ES) <b>Pennsylvania State University, University Park, PA 16802</b>		8. PERFORMING ORGANIZATION REPORT NUMBER	
9. SPONSORING/MONITORING AGENCY NAME(S) AND ADDRESS(ES)		10. SPONSOR/MONITOR'S ACRONYM(S)	
		11. SPONSOR/MONITOR'S REPORT NUMBER(S)	
12. DISTRIBUTION/AVAILABILITY STATEMENT <b>Approved for public release, distribution unlimited</b>			
13. SUPPLEMENTARY NOTES <b>See also ADM001792, International Symposium on Rarefied Gas Dynamics (24th) Held in Monopoli (Bari), Italy on 10-16 July 2004.</b>			
14. ABSTRACT			
15. SUBJECT TERMS			
16. SECURITY CLASSIFICATION OF:			17. LIMITATION OF ABSTRACT
a. REPORT <b>unclassified</b>	b. ABSTRACT <b>unclassified</b>	c. THIS PAGE <b>unclassified</b>	<b>UU</b>
			18. NUMBER OF PAGES <b>6</b>
			19a. NAME OF RESPONSIBLE PERSON

stagnation pressure in the device to levels on the order of 1-5 atm. It is reasonable to use the NS technique for these higher pressure levels.

**TABLE 1. Internal Nozzle Dimension**

length (sub and supersonic parts ):	4930 $\mu m$
inlet height:	600 $\mu m$
throat height:	300 $\mu m$
exit height:	750 $\mu m$
thickness (third dimension):	600 $\mu m$

### 3. NUMERICAL METHODS

The flow parameters are calculated by a 3D DSMC approach for a stagnation pressure of 0.1 atm and by a 3D NS solver for a stagnation pressure level of 0.1 and 5 atm. It must be noted that the calculations of the flow parameters at a pressure level of 0.1atm is challenging for both methods. The flow is sufficiently dense for numerical accuracy to be of concern in a DSMC calculation (the Kn number measured across the wide (third dimension) of the nozzle inlet is 0.01) and it becomes even more dense in the boundary layer close to the cold wall. On the other hand the flow regime is also close to the limits that are solvable by a NS method and probably slip boundary conditions should be used.

The DSMC method is a statistical approach of the Boltzmann equation describing the discrete nature of the gas. The method was proposed by G.A. Bird Ref. [3] and has become the most valuable method for the modeling and simulation of rarefied gases. The SMILE Ref. [4] software, which implements majorant frequency scheme, of Ref. [5], is used in these studies.

Implementation of the DSMC method requires time and space discretization by sufficiently small quantities to insure that the predicted flow parameters correspond to the solution of the Boltzmann equation. Furthermore these numerical parameters are adaptive to the flow gradients and a reasonable number of computational particles must be involved in the calculation in order to obtain a true solution of the Boltzmann equation. The investigation of the influence of numerical parameters of the method on the obtained flow quantities is the goal of this work.

The numerical solution of the Reynolds-averaged Navier-Stokes equations for viscous flow is obtained by use of the GASP Ref. [6] software which utilizes a finite volume discretization of the computational domain. A no-slip boundary condition is used to model the gas-surface interaction. Both subsonic and supersonic parts of the nozzle flow are modeled in the calculations. The nozzle inlet Mach number was chosen to be 0.1 in order to satisfy GASP requirements.

The 3D structural mesh is created and optimized using GRIDGEN Ref. [7] software in order to accommodate the flow gradients. Several steps of the mesh refinement are performed. The entire computational domain is divided into a number of zones and different meshing strategies are used for each zone. Special attention is paid for developing the mesh in the boundary layer and nozzle lip zones where the flow gradients are expected to be large. The mesh structure has been adopted following the flow gradients predicted by each run of the numerical procedure. Again the goal of this investigation is to obtain independence of the predicted flow parameters from further mesh refinement.

### 4. COMPUTATIONAL STRATEGY AND RESULTS

The investigations of the 0.1 atm case by means of the DSMC method and 5 atm case by means of the NS method are now completed with final results obtained. The 0.1 atm NS calculations are currently underway, therefore, the presented results are preliminary.

## 4.1 Direct Simulation Monte Carlo Results

Several calculations have been done with the most intensive ones taking about two weeks to perform on a cluster of 46 Intel Xenon 2.4 GHz processors. The computational time step has been chosen to be the smallest possible for the available machine (single precision) so that its influence on the results can be probably excluded.

The first DSMC calculation has been performed with a reasonable yet relatively small amount of  $\sim 1,300,000$  particles and  $\sim 670,000$  cells. It should be noted that SMILE software adopts the computational grid to the flow gradients while keeping, at the same time, the average number of particles of about 3 to 4 in a computational cell. Therefore, further grid adaptation is only possible by adding more particles to the computational domain. Four computational runs with a gradual increase of the number of particles were performed. The numbers of particles at each run were 1,300,000; 12,200,000; 65,200,000 and 130,000,000. The final increase is only a factor of two only since the limits of the computational resources on the cluster were reached. Figure 2 presents the flow density contours obtained in the cases A and D. Table 2 summarizes the computational scheme parameters for all of the DSMC calculations presented on the figures. Even though the general shape of the number density contours is the same for the both runs, the boundary layer contours in the subsonic part of the nozzle are quite different. The discrepancy between the simulation runs is even more evident in the temperature and flow velocity profiles.

Figure 5 presents translational temperature across the nozzle in the middle of its supersonic part and Fig. 6 presents x-velocity profiles across the nozzle exit. Figures 7 and 8 present translational temperature and the x component velocity along the nozzle centerline respectively. Figures 6 and 8 also shows NS results obtained by Case H for purposes of comparison. The figures 5-8 suggest that a better grid strategy should be employed in future modeling efforts. The following conclusion could be made by analyzing the Figs. 5-8. Even though the essential DSMC requirements for the time step and the number of particles in a computational cell are satisfied in all the calculations, and all the computational runs reach steady state, quantitative and even qualitative changes of the flow parameters are evident when advancing from a low-resolution mesh (Case A) to a higher-resolution mesh (Case D).

## 4.2 Navier-Stokes results

The initial mesh of the presented NS runs has spatial resolution similar to the grid used in the first DSMC calculation (case A). About 750,000 mesh points are deployed in the computational domain and special attention is paid to the meshing of the boundary layer and the nozzle lip regions. The refined mesh structure has about 5,300,000 mesh points Table 3 summarizes the computational scheme parameters for all of the NS calculations.

Figure 3 shows the Mach contours in the XY symmetry plane for the 3D NS calculation for the initial conditions at 0.1 atm. This result was obtained using coarse mesh structure (Case G) It can be seen in the figure that the calculated flow is incorrect, even qualitatively. The boundary layer occupies practically the entire supersonic part of the nozzle. Figure 4 shows distribution of the same parameter obtained using a dense mesh structure (Case H). The quality of the parameter distribution became more reasonable. X-velocity profiles across the nozzle exit and along the nozzle centerline for this case are presented on Figs. 6 and 8 respectively in comparison with the same parameters obtained by DSMC method.

Figure 9-12 present Mach number contours, temperature contours, x-velocity profiles across the nozzle exit and temperature along the nozzle centerline respectively for the inlet pressure of 5.0 atm. The increase of the stagnation pressure makes the conditions more suitable for the NS solver and better results can be expected. It is seen in the figures 9-10 that the contours of parameters are qualitative correct.

Furthermore figures 11-12 show independence of the results obtained for the inlet pressure of 5.0 atm from the computational mesh and from the order of the scheme accuracy. Solution of the first order of accuracy obtained on the coarse mesh structure changes only slightly along with refinement of the mesh and improving the scheme order of accuracy. Unfortunately, a comparison with the DSMC solution for these initial conditions is not possible since the DSMC scheme is prohibitively computationally expensive for such high pressures.

## 4. CONCLUSIONS

The numerical studies of the low Reynolds MEMS flow indicate that the modeling of such flows remains challenging. According to the flow characteristics, a NS solver should be suitable to the modeling of such flows, however, our initial calculations demonstrate that the application of NS to the MEMS flows for transitional Kn numbers is not straightforward. The DSMC modeling is shown to be possible, but the computational cost remains high. It is not clear at this point which method is more applicable for modeling of this type of flows. Further work, in which a NS mesh with a more accurate representation of the flow gradients will be implemented, may reveal better applicability of the NS solver. Slip jump boundary conditions used in NS will allow extend the applicability of the method. Several technical improvements are also planned to make the DSMC method faster and save computational cost.

## 5. ACKNOWLEDGMENTS

The research performed at the Pennsylvania State University was supported by NASA Glenn Research Center under Grant No. NAG3-2590 administered by Mr. Dr. Brian Reed.

## REFERENCES

1. B.D. Reed, W. de Groot, L. Dang, Experimental Evaluation of Cold Flow Micronozzles, AIAA Paper 2001-3521, July 2001.
2. A.A. Alexeenko, D.A. Levin D.A. Fedosov, and S.F. Gimelshein, Coupled Thermal-Fluid Modelling of Micronozzles for Performance Analysis, AIAA Paper 2003-4717
3. Bird G.A., Molecular Gas Dynamics and the Direct Simulation of Gas Flows, Clarendon Press, Oxford, 458pp., 1994.
4. M.S. Ivanov, S.F. Gimelshein, Current Status and Prospects of the DSMC Modeling of Near-Continuum Flows of Non-reacting and Reacting Gases, Rarefied Gas Dynamics, 23<sup>rd</sup> Int. Symp., AIP Conference Proceedings, Vol 663, pp. 339-348, 2003.
5. M.S. Ivanov and S.V. Rogasinsky, Analysis of numerical techniques of the Direct Simulation Monte Carlo method in the rarefied gas dynamics., Sov. J. Num. Anal. Math. Modelling, 3(6):453-456,1988.
6. General Aerodynamic Simulation Program, Computational Flow Analysis Software for the Scientist and Engineer, Gasp Ver. 3, User's Manual, Aerosoft Co., Blackburg, VA, May 1996.
7. Gridgen User Manual, Pointwise, Inc.,1999.

**TABLE 2. DSMC scheme parameters**

Case	Number of particles	Number of cells
A	1,300,000	670,000
B	12,000,000	5,600,000
C	65,000,000	27,000,000
D	130,000,000	52,000,000

**TABLE 3. NS scheme parameters**

Case	Mesh points	Order of accuracy	Pressure [atm]
E	750,000	1	5.0
F	5,300,000	2	5.0
G	750,000	1	0.1
H	5,300,000	1	0.1

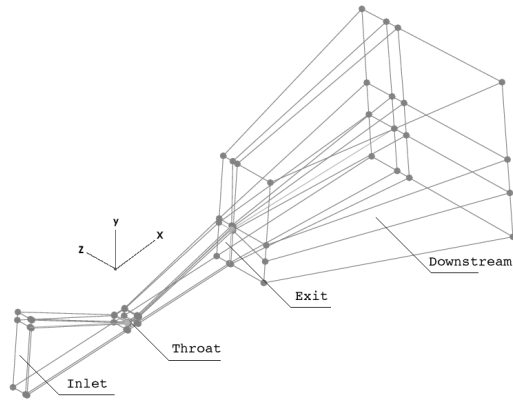


FIGURE 1. Computational Domain for a series of NS calculations

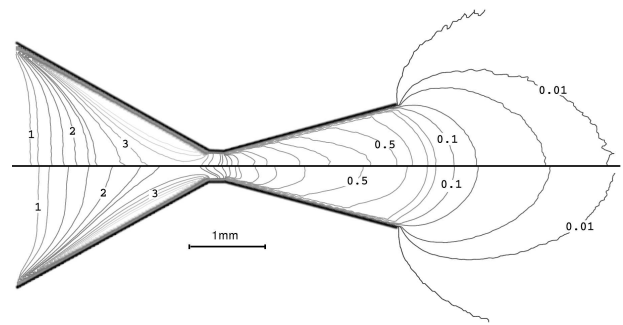


FIGURE 2. Number density contours ( $1 = 5.0 \times 10^{23}$ ) top: case A, bottom: case D

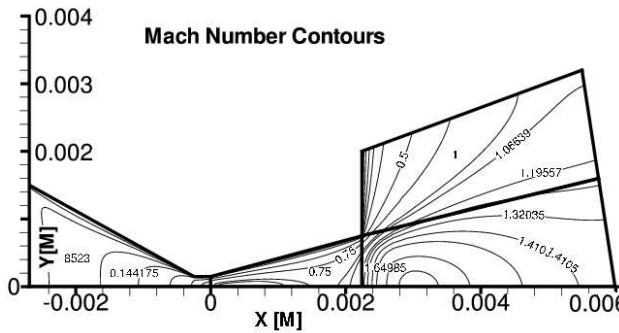


FIGURE 3. Mach number contours, Case G

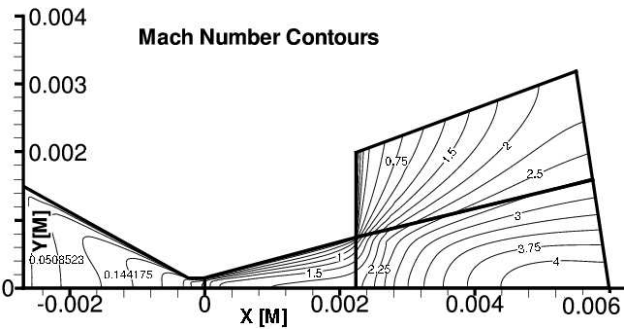


FIGURE 4. Mach number contours, Case H

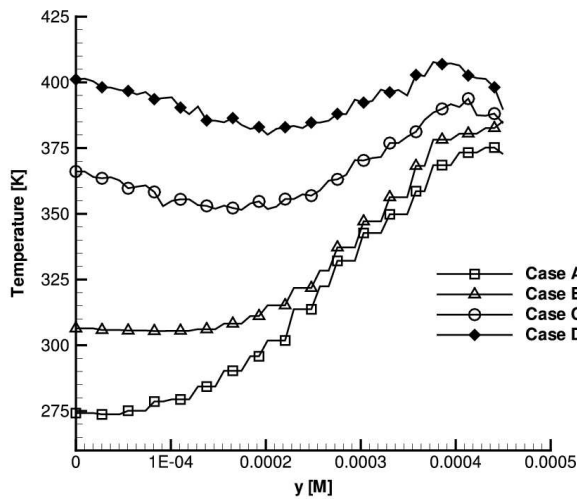


FIGURE 5. Translational temperature across the nozzle in the middle of the supersonic part. The nozzle axis is located at  $x=0$ .

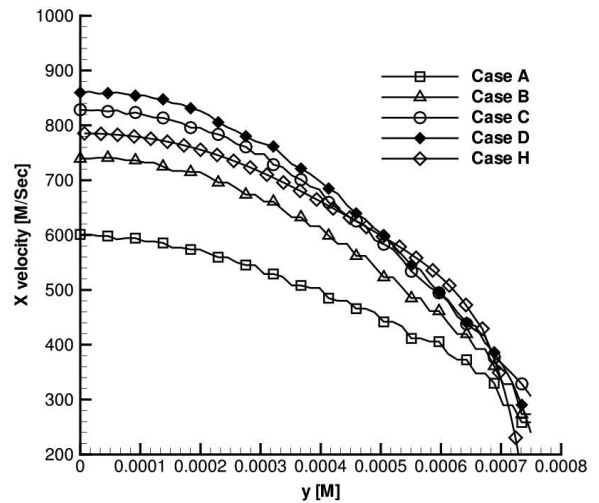


FIGURE 6. X-velocity profiles across the nozzle exit. The nozzle axis is located at  $x=0$ .

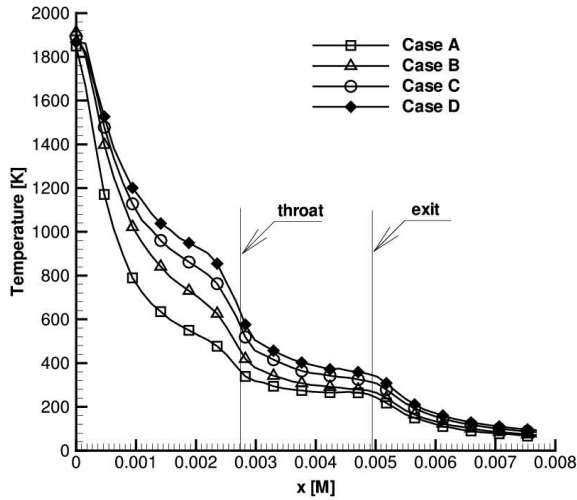


FIGURE 7. Translational temperature along the nozzle centerline.

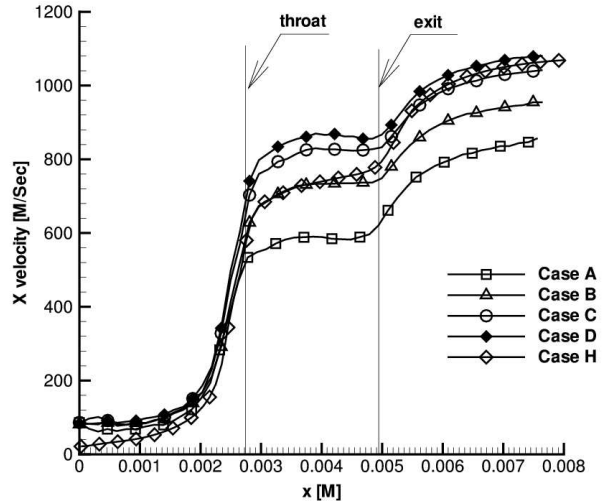


FIGURE 8. X-velocity along the nozzle centerline.

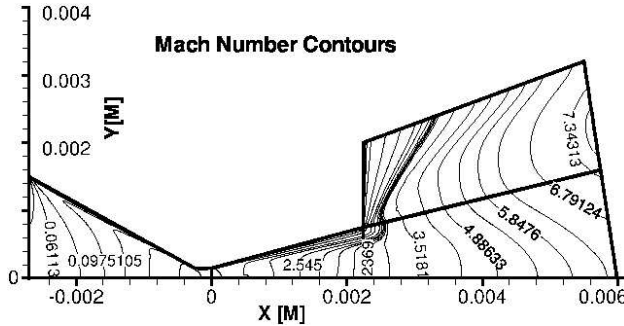


FIGURE 9. Mach number contours, Case F

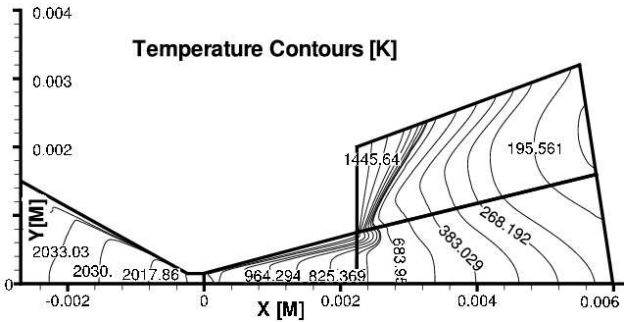


FIGURE 10. Temperature contours, Case F

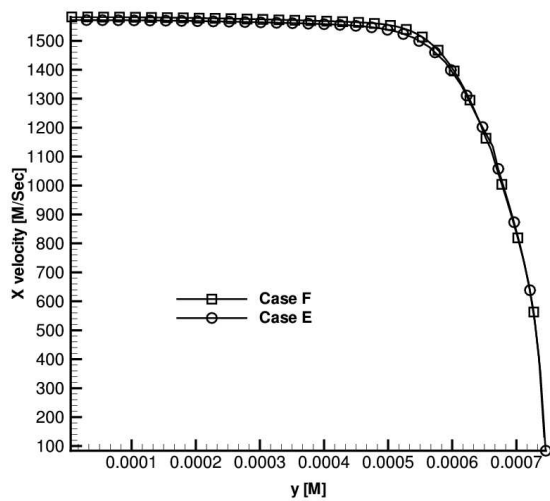


FIGURE 11. X-velocity profiles across the nozzle exit. The nozzle axis is located at  $x=0$ .

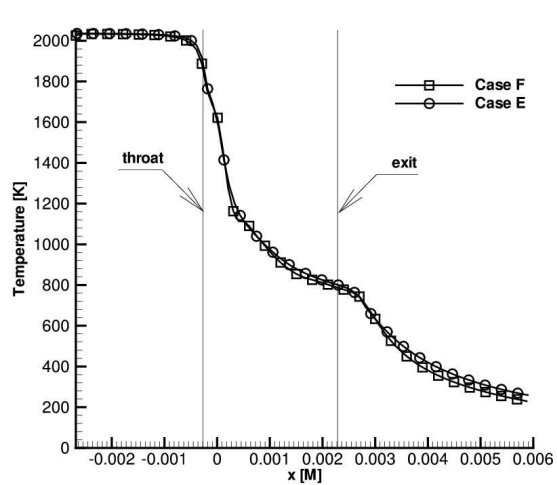


FIGURE 12. Temperature along the nozzle centerline.